

Reef communities show predictable undulations in linear abundance size spectra from copepods to sharks

Freddie J. Heather  | Rick D. Stuart-Smith | Julia L. Blanchard | Kate M. Fraser |
Graham J. Edgar

Institute for Marine and Antarctic Studies,
University of Tasmania, Hobart, TAS,
Australia

Correspondence

Freddie Heather, IMAS Taroona, 15-21
Nubeena Cres, Taroona, Hobart, TAS
7053, Australia.
Email: freddieheather@gmail.com

Funding information

Australian Research Council, Grant/Award
Number: LP150100761

Editor: David Mouillot

Abstract

Among the more widely accepted general hypotheses in ecology is that community relationships between abundance and body size follow a log-linear size spectrum, from the smallest consumers to the largest predators (i.e. ‘bacteria to whales’). Nevertheless, most studies only investigate small subsets of this spectrum, and note that extreme size classes in survey data deviate from linear expectations. In this study, we fit size spectra to field data from 45 rocky and coral reef sites along a 28° latitudinal gradient, comprising individuals from 0.125 mm to 2 m in body size. We found that 96% of the variation in abundance along this ‘extended’ size gradient was described by a single linear function across all sites. However, consistent ‘wobbles’ were also observed, with subtle peaks and troughs in abundance along the spectrum, which varied with sea temperature, as predicted by theory relating to trophic cascades.

KEYWORDS

body size, epifauna, power law, secondary structure, sine curve, sinusoidal, size spectrum, size-based, UVC sampling bias

INTRODUCTION

The body size of an organism is often regarded as the single most important factor determining how it interacts with its environment (Brown et al., 2004; Gillooly et al., 2002; Peters, 1983; Schmidt-Nielsen & Knut, 1984). At the community level, the relationship between an individual's body size and abundance can provide important insights into how energy, and hence biomass, moves through the food chain (Brown & Gillooly, 2003; Trebilco et al., 2013). Similar biomass across logarithmic body size classes is often observed in marine communities (Sprules & Barth, 2016), which equates to decreasing abundance with increasing body size, termed the abundance size spectrum (Trebilco et al., 2013).

In marine communities, the faunal abundance size spectrum is often described by a linear function on the log–log scale. The intercept and slope of this function can provide information about nutrient availability (e.g.

Boudreau & Dickie, 1992; Sprules & Munawar, 1986), human disturbance (Dulvy et al., 2004; Graham et al., 2005; Shin et al., 2005; Wilson et al., 2010) and feeding strategies of the individuals (Robinson et al., 2016) in the community. In pelagic systems, a consistent size spectrum is commonly observed, often attributed to strict size-based predation (Jennings et al., 2001) and trophic level inefficiencies (Lindeman, 1942), in combination with the relationship between body size and metabolic rate (Kleiber, 1932).

Deviations from size spectrum linearity, for example, peaks of abundance at specific body sizes, have been described in lake systems (e.g. Sprules et al., 1983), intertidal (Schwinghamer, 1981) and subtidal (Edgar, 1994) benthic communities. Schwinghamer (1981) attributed these peaks in abundance to the physical environment, whereby sediment grain size created size-based habitat niches. Rogers et al., (2014) showed a similar pattern on coral reefs, whereby deviations from linearity reflected

habitat complexity via habitat refugia for prey. These abundance peaks have also been attributed to trophic interactions, with early studies proposing that peaks in abundance correspond to outcomes of interacting functional groups (Dickie et al., 1987). More recent work has shown mechanistically that peaks in abundance can arise from bottom-up (e.g. food limitation) and top-down (e.g. predation mortality) trophic cascades (Andersen & Pedersen, 2010; Benoît & Rochet, 2004; Rossberg et al., 2019). While a combination of these influences is likely, no clear consensus exists on the drivers of these nonlinear patterns in faunal size spectra.

Reef studies tend to focus on fishes, where observed size spectra are often unimodal, with a peak in abundance at a small to intermediate body size (e.g. Ackerman et al., 2004). Due to theoretical expectations of decreasing abundance with body size, and the potential for under-sampling smaller individuals, many reef size spectra have routinely excluded individuals less than the modal size, or equivalent size, from the linear modelling analyses (Heather et al., 2021; Robinson et al., 2017; Trebilco et al., 2015; Wilson et al., 2010) (See Figure 1a). Ignoring the small fishes and fitting a linear model to the size spectrum has the benefit of simplicity and has also been shown to be useful in detecting fishing pressure on reefs (Robinson et al., 2017). These studies have typically used visual survey methods to collect data, which are known to under-represent densities of some species (Bozec et al., 2011), particularly for small (Ackerman & Bellwood, 2000), cryptic (Stewart & Beukers, 2000; Willis, 2001) and nocturnal fishes (Azzurro et al., 2007). For example, Ackerman and Bellwood (2000) found their

visual survey methods underestimated the abundance of reef fishes <5 cm by 75%.

In this study, we use individual body size data spanning 0.125 mm to 2 m across 28° of latitude to systematically test the a) generality of a linear size spectrum on reefs and b) the presence and cause of the dip in abundance at the small to medium size classes. We applied two distinct methods to collect field data on abundance and size of consumer taxa on 45 reefs from 14.7°S to 43.3°S along the eastern coastline of Australia, including macroalgal covered temperate rocky reefs and coral reefs in the tropics. One method involved sampling of animals associated with benthic habitat ('epifauna': 0.125 mm to 22 mm body size), while the other involved visual census of larger mobile invertebrates and fishes along underwater transect lines ('visual survey data': 0.01 m to 2 m body size). Together these approaches provided density estimates for all mobile species that could readily be surveyed by divers at a given patch of reef.

The inclusion of invertebrates in smaller and overlapping size classes to the fishes allows for testing of three hypotheses about causes of the abundance dip in the size spectrum observed in reef fishes (Figure 1a): (1) It arises from disproportionate under-sampling of small fishes in visual census surveys, as has been assumed in previous studies the rationale for removal of this part of the spectrum. This would be seen through a 'gap' in the size spectrum (Figure 1b); (2) It is part of a consistent curve in the overall size spectrum of reef consumers, which would be seen in a continuous, but curved size spectrum (Figure 1c); 3) It is an artefact of only considering fishes in isolation, and that part of the spectrum is filled by invertebrates that

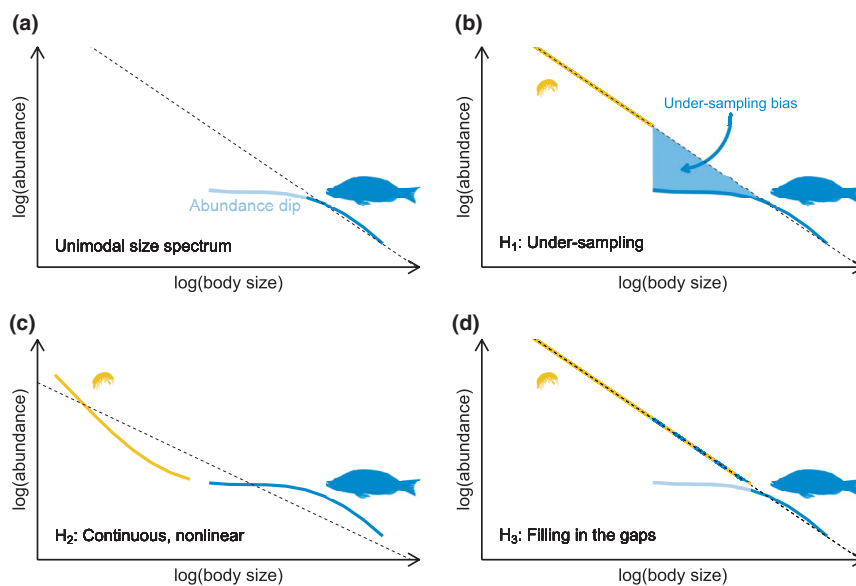


FIGURE 1 Conceptual diagram showing the dip in abundance of small fishes typically observed in studies of reef fish size structure (a), and three alternative hypothetical spectra (b–d) that account for the pattern observed in (a). Where the size spectrum is unimodal (a), a linear function is generally fitted to the descending limb (darker blue), with smaller size classes assumed to be under-sampled (lighter blue) and excluded. A linear overall size spectrum with a substantial gap (b) would indicate that under-sampling is likely to be the cause, while a continuous curve with a smooth transition through the size classes where the fishes and invertebrates overlap (c) would suggest that ecological interactions drive a real nonlinearity. A continuous strongly linear spectrum (d) would indicate that epifaunal invertebrates fill the gaps left by fishes

are usually neglected (Heather et al., 2021). This would be seen by a strongly linear overall spectrum (Figure 1d). These competing hypotheses each assume the overarching principles of size-based feeding (Jennings et al., 2001) and transfer inefficiency (Lindeman, 1942) are operating in reef systems, which have been well supported by previous studies (see Sprules & Barth, 2016).

METHODS

Survey data

Data collection was performed using two distinct methods: (1) Collection of benthic habitat samples with associated invertebrate epifauna and (2) underwater visual surveys of fishes and large mobile macro-invertebrates. Together, these datasets allowed construction of size spectra from small meiofaunal invertebrates (predominantly harpacticoid copepods, Fraser et al., (2021)) to the largest fishes including sharks (Edgar et al., 2014).

Epifauna were sampled from 45 sites spanning the eastern coast of Australia, from tropical (Lizard Island; 14.7°S) to temperate (Southern Tasmania; 43.3°S) reefs, between the years of 2015 and 2018. Sample collection involved firstly characterising the habitat at the site by taking 20 evenly spaced photographs of benthos and substrata along each of two 50 m survey transects. Photographs were taken from approximately 50 cm above the substrata to depict approximately 30 × 30 cm of seabed. These photographs were assessed to derive an estimate of the relative abundance of different habitat types at each site (Cresswell et al., 2017). Habitat selected for sampling was then covered with a 25 × 25 cm grid-marked quadrat and photographed in situ to quantify its planar area. Habitat and epifaunal samples were bagged in situ after detachment by removing soft habitat (e.g. macroalgae, sponges) with a knife and hard coral habitat with a chisel (Fraser et al., 2021). Habitat that could not easily be removed (e.g. turfing algae, encrusting coral) was vacuum sampled using a venturi airlift. Each habitat sample was flushed with freshwater to remove mobile epifauna, which were then passed through a set of logarithmic ($\log \text{ base } = \sqrt{2}$) mesh size sorting sieves. Animals retained on each sieve were counted and identified to the highest possible taxonomic resolution. For more detailed methodology, see Fraser et al., (2021). Abundance of epifauna by size and taxa was standardised to 1 m² planar area by multiplying the number of individuals per unit area of sampled habitat type with transect area photographed comprising this habitat type.

Fish and large mobile invertebrate species (>2.5 cm maximum recorded length) were surveyed using the standardised Reef Life Survey visual census methods (Edgar & Stuart-Smith, 2014; Edgar et al., 2020, see also <https://reeflifesurvey.com/>), in which SCUBA divers swim along a 50 m transect line and record all fishes

and invertebrates observed within 5 and 1 m wide belts respectively. Divers estimate body size of animals observed to the closest of 13 size categories (2.5, 5, 7.5, 10, 12.5, 15, 20, 25, 30, 35, 40, 50 and 62.5 cm) or to the nearest 12.5 cm for body sizes greater than 62.5 cm. Potential biases in visual data collected using this methodology are discussed by Edgar et al., (2020). For large mobile invertebrates, of which body size was not always estimated at the time of observation, body size was estimated using the lognormal probability distribution of body size based on the asymptotic size of the species (see Heather et al., 2021). Densities of fishes and invertebrates were standardised to abundance per m² by dividing the individual number counts by the respective area surveyed.

Combining the datasets

The body size of individuals from the two datasets overlapped at some sites. To combine these data, we binned both datasets into log bins with a base of $\sqrt{2}$ and summed the abundance of the bin to obtain a total abundance within the size bin. A log base of $\sqrt{2}$ was chosen as this represented the logarithmic sieve mesh sizes of the epifaunal sampling. Normalised density was calculated as the density (abundance per m²) divided by the width of the body size bin (Platt & Denman, 1977).

Fitting nonlinear size spectra

Due to clear sinusoidal patterns in the residuals of linear functions between log body size and log abundance, we fitted a nonlinear size spectrum model proposed by Rossberg et al., (2019) (Equation 1). This model included both a linear function with an additional sinusoidal function to allow for the quantification of both the linear and secondary structure aspects of the size spectrum.

$$\log(N) = \beta_0 + \lambda \log(L) + A \sin\left(\frac{2\pi \log(L)}{D} - P\right) \quad (1)$$

Where, N is the normalised density (m⁻²), L is the middle of the size bin (mm), β_0 is the size spectrum intercept, λ is the slope and A, D and P represent the amplitude, wavelength and phase of the sine wave respectively. The size spectrum model (Equation 1) was fitted using the 'nlrq' function (Koenker & Park, 1994) in R (R Core Team, 2020). The amplitude (A) represents the 'strength' of the sine wave, and therefore the deviation from linearity in the size spectrum. Rogers et al., (2014) used the pareto distribution to detect deviations from linearity, due to the body size data being resolved to the individual level rather than in logarithmic size bins. Individual level body size data would allow for the detection of finer-scale deviations from linearity; however, this was not feasible in this study due to the inherent binning

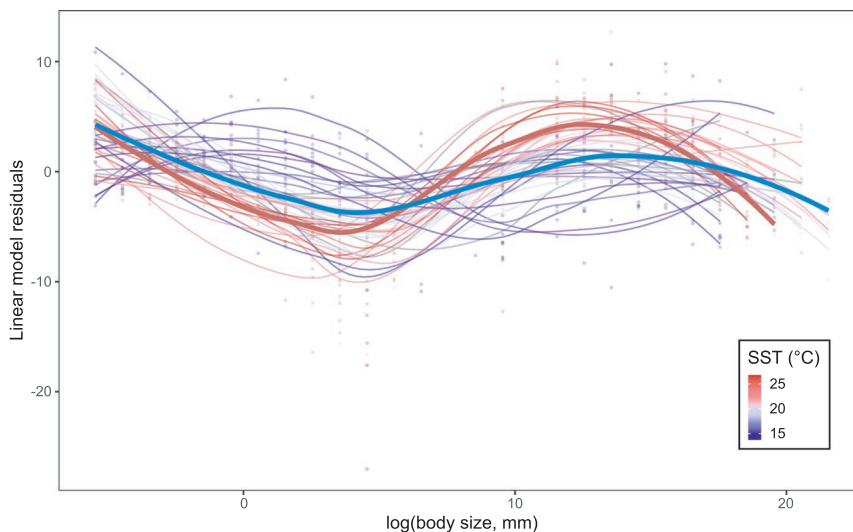


FIGURE 2 Sinusoidal patterns in the residuals of the linear model of the size spectrum. Each line represents a LOESS fit for a given site. Each thin line represents a site, with the colour of line representing the mean annual sea surface temperature (SST) at the site. The two thick lines represent the combined LOESS fit for tropical (red) and temperate sites (blue)

nature of data collection (both sieving and visual survey methods). The ratio of abundance from the top of one peak to the bottom of a trough was calculated as the log base to the power of two times the amplitude ($\sqrt{2}^A$). The body size ratio of individuals occupying neighbouring peaks was calculated as the log base to the power of the wavelength ($\sqrt{2}^D$), and the distance between consecutive peaks and troughs was, therefore, estimated as the log base to the power of half the wavelength ($\sqrt{2}^{\frac{D}{2}}$). If the peaks and troughs in the size spectrum are driven by trophic cascades, then the distance between consecutive peaks and troughs ($\sqrt{2}^{\frac{D}{2}}$) relates to the ratio between the body size of predators and prey.

Due to the difficulty of interpreting the phase parameter (P) of the nonlinear size spectrum when the wavelength (D) is not fixed (Rossberg et al., 2019), we identified the body size in which local peaks and troughs occurred in the size spectrum model using the ‘optimize’ function in R (R Core Team, 2020).

Hypothesis testing

To test the three competing hypotheses (Figure 1), we fit three models at each site to the combined dataset (epifaunal and visual survey data); (1) a linear model, (2) a nonlinear model (Equation 1) and (3) a linear model excluding size classes within the ‘abundance dip’ (Figure 1a). If the inclusion of the epifaunal data fills the size classes with reduced relative abundance (i.e. the abundance dip) (Hypothesis 3, Figure 1d), then we would expect the resultant size spectrum to be best described by a simple linear model at the site (Equation S1). If the removal of the data points corresponding to the size bins within the abundance dip (defined as visual survey data size classes smaller than the modal body size class) results

in an overall better linear model (Equation S1) fit than when all size bins are included, this supports our first hypothesis (Figure 1b) that these size classes are potentially under-sampled. If the nonlinear model provides a better fit than the other two linear models, this supports the second hypothesis; that the inclusion of epifauna results in a size spectrum with the region referred to as the abundance dip being an inherent part of an overall nonlinear size spectrum (Hypothesis 2, Figure 1c). The goodness-of-fit of the three models was determined by the Akaike information criterion (AIC) value (Akaike, 1974) (see Supplementary material S5).

Environmental covariates

We fitted a series of maximal linear models (Supplementary material S4) to identify the most important covariates in estimating the parameters of the size spectrum model (Equation 1). These site covariates included mean sea surface temperature (°C), mean chlorophyll level (mg m^{-3}), phosphate and nitrate levels (mmol l^{-1}), all extracted from Bio-ORACLE, (Tyberghein et al., 2012) and categorical indices of wave exposure, habitat relief, currents and reef floor slope, scored on a 1–4 scale by divers at the survey sites. Details on these environmental variables can be found in Supplementary S2. Using a best subset regression approach (Hebbali, 2020), we selected the environmental variables that minimised the AIC value (Table S2).

RESULTS

When combining the epifaunal and visual survey datasets, 96% of the variation in logarithmic normalised

abundance (N) was explained by a linear function of logarithmic body size (L) (linear regression: $\log(N) \sim \log(L)$; all sites combined, Equation S2). More variation was explained when combining these datasets (Adjusted $R^2 = 95.8\%$), than when a linear model was fitted to the datasets separately (Epifaunal data, Adjusted $R^2 = 90.1\%$; Visual survey data, Adjusted $R^2 = 84.3\%$). At the majority of sites we observed no individuals in the range of 5–22 mm (size bins $\sqrt{2}^5$ to $\sqrt{2}^8$ in Figure S1).

Clear sinusoidal patterns were present in the residuals of the linear model fits (Equation S1) (Figure 2). At 41 of the 45 sites (Figure 4), the nonlinear size spectrum model (Figure 3, Equation 1, Figure S2) provided a better fit (lower AIC) than either a linear model (Equation S1) incorporating all data (epifaunal and visual survey) and a linear model (Equation S1) with all data but excluding the size bins making up the visual survey 'abundance dip'. At three of the 45 sites (Figure 4, Table S3), the best fitting model was the linear model excluding size classes within the abundance dip (Figure 4, Table S3); suggesting potential under-sampling of these size classes at these three sites. The size spectrum of one site (EMR47, Figure S1, Figure 4, Table S3) was best described by a linear function. There was no apparent abundance dip at

this site, which therefore did not support any of the three hypotheses.

The mean community level predator-to-prey size ratio, calculated as the log base to the power of half the wavelength $\sqrt{2}^{\frac{\lambda}{2}}$, was estimated to be 28.1 (± 10.3 , 95% confidence interval). That is, a predator is expected to be 28.1 times the body length of its prey.

The fitted nonlinear size spectrum parameter values at the site were regressed against the site-level environmental variables (see Table S2 and Equations S3–S6 for the full fitted models). These combinations of environmental variables explained 31% of the variation (as determined by the R^2 value of Equation S3) in size spectrum amplitude, 19% of variation in size spectrum wavelength, 60% of the variance in the size spectrum slope and 35% of the variance in the body size where relative peak abundance occurs (see peaks in Figure 2).

The slope of the size spectrum (λ) increased (i.e. became shallower) with increasing site mean sea surface temperature (SST). The position of the peak abundance was also dependent on the site SST, whereby the peak abundance occurred at around 19.8 cm in temperate sites compared to around 7.4 cm at tropical sites (Figure 2).

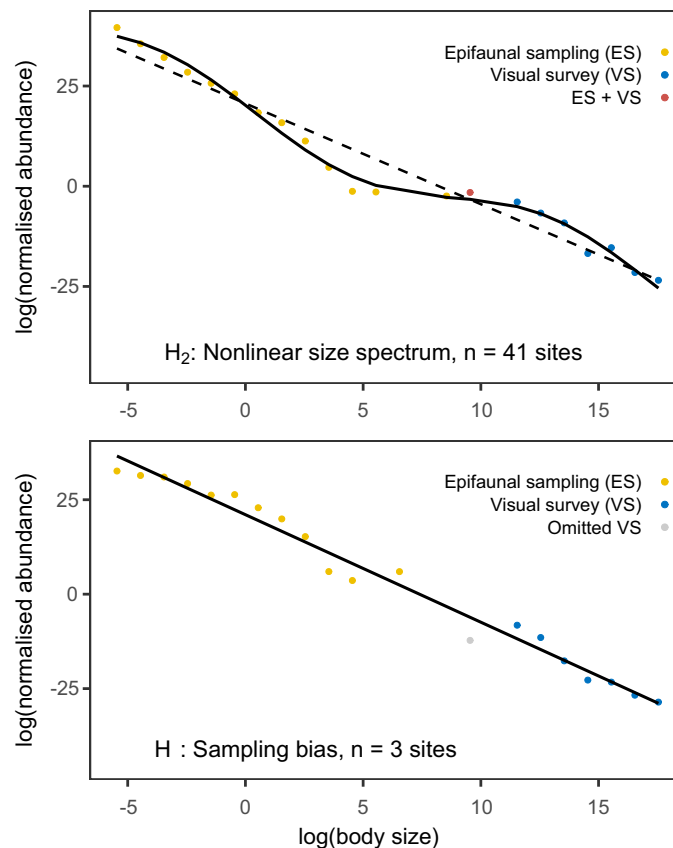


FIGURE 3 Abundance size spectra for two example reefs, each providing support for one of the proposed hypotheses. The upper panel shows the size spectrum of a single reef (GBR27) where a nonlinear continuous size spectrum model better describes the community than a linear model, this was observed in 41 of the 45 sites. The lower panel shows an example reef (NIN-S1) where there is potentially under-sampling of the smallest body size class of the visual survey data. The datapoint colour represents the sampling method of the individuals that make up the size class

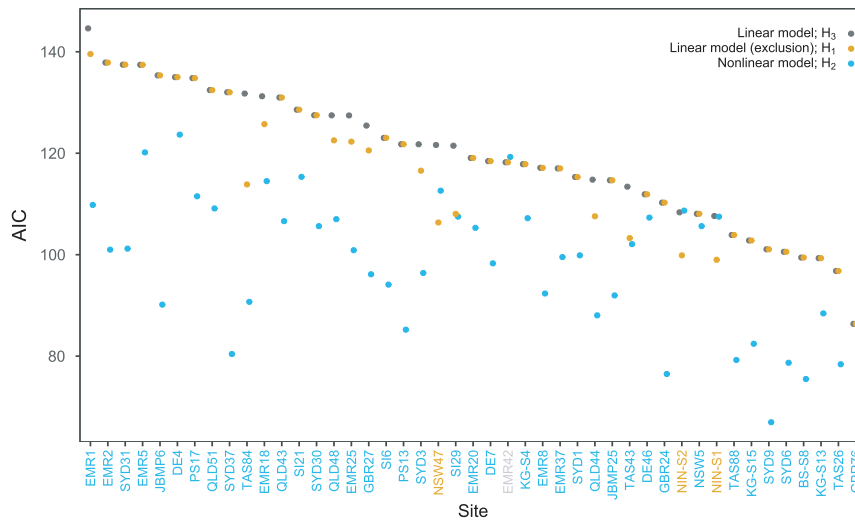


FIGURE 4 Comparison of the goodness-of-fit of three models fit to 45 reef size spectra; the Akaike information criterion (AIC) value for a linear model (dark grey points), a linear model excluding size bins within the abundance dip (orange points) and a nonlinear sinusoidal model (blue points). Points have been horizontally jittered to avoid data point overlap. Each model provides support for one of three hypotheses (H_1 , H_2 and H_3). The colour of the x-axis text refers the best fitting model (lowest AIC) at the site and the hypothesis it supports, which are ordered by linear model (dark grey) AIC values for illustrative purposes. One site (EMR42, light grey text) does not support any of the three hypotheses. Geographical locations of the sites can be found in Figure S1

DISCUSSION

While there was an extremely strong linear component to the size spectra, the addition of a sinusoidal component resulted in better model fitting at 41 of the total 45 sites. This supported our second hypothesis (Figure 1c) that the abundance dip commonly assumed to be solely a sampling artefact is part of a nonlinear size spectrum. A few sites nevertheless provided evidence of under-sampling of small- to medium-sized fauna (e.g. NIN-S1, NIN-S2, NSW47, lower panel in Figure 3). Thus, some support for the first hypothesis (Figure 1b) also exists, with under-sampling of smaller sized fishes indicating that the visual methods used cannot cover fishes with equal probability of observation along the size spectrum. Regardless, the data suggest that under-sampling is not likely the primary reason for the non-linearity in reef fish size structure, potentially affecting conclusions of previous studies where smaller size classes had been removed.

The dip in abundance in the range of 2.5 to 10 cm for visual survey data observed here (blue datapoints in Figure S1, see also Figure 1a) is consistent with the patterns observed in previous reef size spectra studies (Ackerman & Bellwood, 2000; Ackerman et al., 2004). Ackerman et al., (2004) used rotenone poisoning sampling to comprehensively sample all reef fauna and observed a similar dip in abundance in this size range. Our results also suggest that the dip in abundance is a true feature in an overall size spectrum (Figure 1) that is nonlinear (i.e. supporting H_2 , Figure 1c). We also note that the complete absence of individuals in the size bins ranging 5–22 mm was observed at many sites (Figure S1). This absence is likely due to individuals missed in both

sampling methods, for example small mobile individuals, missed by both habitat-associated epifaunal sampling, and below the visible limit of visual surveys.

Wave-like patterns in size spectra have been previously observed in lake studies (e.g. Boudreau & Dickie, 1992; Sprules et al., 1983), and have been reproduced in mechanistic modelling studies (e.g. Andersen & Pedersen, 2010; Rossberg et al., 2019). The mechanistic approaches indicate trophic cascades driven by fishing pressure (Andersen & Pedersen, 2010) and nutrient enrichment (Rossberg et al., 2019) can result in wave-like patterns in size spectra. Both studies found that a combination of bottom-up (food availability) and top-down (predation mortality) pressures drove the observed patterns. Further, both studies found wave amplitude to increase with body size (i.e. greater linearity in the size spectrum at smaller body sizes), similar to the patterns observed here (Figure 3). This could be formally tested with a model that allows amplitude to vary with body size; however, this was not applied here due to potential for overparameterisation of the model (see also Rossberg et al., 2019). A test to assess whether nutrient enrichment drives sinusoidal patterns in lakes (Rossberg et al., 2019) requires a greater range of available nutrients (phosphates and nitrates) than was available at the reef sites in this study. If the sinusoidal patterns observed in this study are driven by trophic interactions, we would expect the distance between peaks and troughs to correspond to a mean predator-to-prey size ratio (PPSR) at the community level. Using the wavelength to calculate PPSR, we estimated a mean community PPSR of 28.1, which corresponds to a predator-to-prey mass ratio (PPMR) of $10^{4.3}$ ($=28.1^3$; if we assume isometric growth, $W \propto L^3$), which is consistent with previous estimates of community-level

PPMR (Trebilco et al 2013), further supporting the hypothesis that these sinusoidal patterns are driven by trophic interactions. A dietary study of 88 seagrass inhabiting fishes found predator length to be 13.3x prey length on average, suggesting slightly higher community PPMR on reefs than in seagrass habitats (Edgar & Shaw, 1995).

Another theory explaining nonlinearity in size spectra assumes that habitat complexity provides refugia that favour particular body sizes (e.g. Rogers et al., 2014). The fact that we observed no significant relationship between the survey site relief (a broad-scale measure of habitat complexity) and the size spectrum amplitude (A in Equation 1; a measure of nonlinearity) does not necessarily disprove this theory. Complex habitats are likely to provide a wide range of refugia of varying scales (Hixon & Beets, 1989, 1993; Menge & Lubchenco, 1981; Shulman, 1985) and associated potential niches. Site relief was classified categorically into four levels to describe the broad-scale habitat structure, but these categories would unlikely encompass the finer-scale crevices used as prey refugia. Further, wave amplitude is a measure of the strength of the sine curve, not necessarily a measure of fine-scale deviations from linearity that would be expected from fine-scale habitat complexity. Therefore, the potential mismatch in the broader scale of the relief measures and the finer scale of prey refugia may result in their non-significant relationship observed here. Based on the observed peaks in the size spectrum ranging from 7 to 20 cm, one might hypothesise that refugia for fishes in this size range may be most important, and that smaller refugia in tropical areas support peaks in abundance at smaller sizes than on temperate reefs. The latter is plausible with more finer scale complexity likely among the coral structures on tropical reefs compared to the cover provided by kelps on a rocky base in temperate zones (see below). If the wave amplitude (A) is primarily driven by alternative mechanisms (such as trophic cascades), then analysing the residuals of this nonlinear sinusoidal model may identify a 'tertiary structure' of the size spectrum, potentially driven by finer-scale drivers, such as habitat niches and refugia.

Environmental variables explained a large portion of variability in the size spectra; both the linear (λ) and nonlinear components (A , D and position of peak abundance). Figure 2 indicates that the peak in abundance occurs at larger body sizes in cooler sites compared to warmer sites; using equation S6, we estimate a relative peak in abundance at 7.4 cm with 14°C SST, while a peak at 19.8 cm with 26°C SST (Figure S3). These peaks approximately correspond to the mean body size of the dominant large invertebrate-feeding fishes in temperate regions (e.g. wrasses) and the sometimes hyper-abundant small planktivorous fishes on coral reefs. Numerous explanations potentially account for latitudinally dependent body size preference. Firstly, the dominant energy pathways may vary with latitude, whereby a higher

mean PPMR in temperate reefs leads to less energy lost through trophic inefficiencies and therefore a peak in abundance at larger body sizes. As described above, habitat composition also varies latitudinally and has been shown to play an important role in latitudinal variation in the body sizes of the smallest invertebrates studied here (Fraser et al., 2021; Yamanaka et al., 2012).

Size spectra are widely used as ecological indicators of reef health, for detecting and quantifying ecosystem disturbances such as fishing pressure (Dulvy et al., 2004; Graham et al., 2005; Robinson et al., 2017; Wilson et al., 2010). This application of empirical size spectra as ecological indicators often relies on the assumption that relationships between log abundance (or biomass) and log body size are linear (Dulvy et al., 2004; Graham et al., 2005; Nash & Graham, 2016). Here, we show that 96% of the variation in log abundance can be explained by a linear function of log body mass in individuals ranging from 0.125 mm to 2 m, irrespective of taxonomy or location. Our detailed empirical support for consistency of marine size spectra supports the generality of early conjectures of linear size spectra holding from 'bacteria to whales' (Sheldon et al., 1972). However, in order to use size spectra as ecological indicators for reefs, we must identify a counterfactual baseline representing an 'unimpacted' reef, from which to compare (Jennings & Blanchard, 2004; Petchey & Belgrano, 2010).

Although we observed remarkable consistency in the linearity of the size spectra, subtle nonlinearities are evident. These sinusoidal nonlinearities are similar to those previously observed (e.g. Sprules et al., 1983) and modelled (Rossberg et al., 2019) in lake ecosystems. Whether the inflections reflect disturbances to reefs or are an inherent part of reef size spectra remain speculative. While temperature was found here to be a strong driver of sinusoidal patterns, this factor is likely related to multiple interacting direct and indirect effects on body size, including through changes in habitat composition (Fraser et al., 2021). Trophic cascades potentially also contribute to inflections (Andersen & Pedersen, 2010; Rossberg et al., 2019). Mechanistic models trained with empirical data are needed to test this hypothesis and to identify the main drivers of the nonlinear patterns. Data presented here for remote highly protected reefs (e.g. Middleton Reef, 'EMR') provide a baseline for reef size spectra, and for their expanded use as ecological indicators of reef health.

ACKNOWLEDGEMENTS

This research was supported by the Marine Biodiversity Hub, a collaborative partnership supported through funding from the Australian Government's National Environmental Science Program, and used the NCRIS-enabled Integrated Marine Observing System (IMOS) infrastructure for database support and storage. This research was also made possible by funding of the Australian Research Council (ARC), and the data from

the Reef Life Survey Foundation. The authors also thank data support from Antonia Cooper, Just Berkhout, Scott Ling, Ella Clausius and Elizabeth Oh.

AUTHORSHIP

FH and GE conceptualised the study, FH designed the analysis, analysed the data and led the writing of the manuscript. KF performed epifaunal sampling. All authors contributed to critical feedback, interpretation and substantial revisions of the manuscript.

PEER REVIEW

The peer review history for this article is available at <https://publons.com/publon/10.1111/ele.13844>.

DATA AVAILABILITY STATEMENT

Code for the analysis, and to recreate all figures, is available at https://github.com/FreddieJH/sinusoidal_size_spec. Data used in this study are available at <https://doi.org/10.5281/zenodo.4953088>.

ORCID

Freddie J. Heather  <https://orcid.org/0000-0002-1650-2617>

REFERENCES

- Ackerman, J.L. & Bellwood, D.R. (2000) Reef fish assemblages: a re-evaluation using enclosed rotenone stations. *Marine Ecology Progress Series*, 206(1954), 227–237.
- Ackerman, J.L., Bellwood, D.R. & Brown, J.H. (2004) The contribution of small individuals to density-body size relationships: examination of energetic equivalence in reef fishes. *Oecologia*, 139(4), 568–571.
- Akaike, H. (1974) A new look at the statistical model identification. *IEEE Transactions on Automatic Control*, 19(6), 716–723. <http://ieeexplore.ieee.org/document/1100705/>.
- Andersen, K.H. & Pedersen, M. (2010) Damped trophic cascades driven by fishing in model marine ecosystems. *Proceedings of the Royal Society B: Biological Sciences*, 277(1682), 795–802. <https://royalsocietypublishing.org/doi/10.1098/rspb.2009.1512>.
- Azzurro, E., Pais, A., Consoli, P. & Andaloro, F. (2007) Evaluating day-night changes in shallow Mediterranean rocky reef fish assemblages by visual census. *Marine Biology*, 151(6), 2245–2253. <http://link.springer.com/10.1007/s00227-007-0661-9>.
- Benoit, E. & Rochet, M.J. (2004) A continuous model of biomass size spectra governed by predation and the effects of fishing on them. *Journal of Theoretical Biology*, 226(1), 9–21.
- Boudreau, P.R. & Dickie, L.M. (1992) Biomass spectra of aquatic ecosystems in relation to fisheries yield. *Canadian Journal of Fisheries and Aquatic Sciences*, 49(8), 1528–1538.
- Bozec, Y.-M., Kulbicki, M., Laloë, F., Mou-Tham, G. & Gascuel, D. (2011) Factors affecting the detection distances of reef fish: Implications for visual counts. *Marine Biology*, 158(5), 969–981.
- Brown, J.H. & Gillooly, J.F. (2003) Ecological food webs: High-quality data facilitate theoretical unification. *Proceedings of the National Academy of Sciences*, 100(4), 1467–1468.
- Brown, J.H., Gillooly, J.F., Allen, A.P., Savage, V.M. & West, G.B. (2004) Toward a metabolic theory of ecology. *Ecology*, 85(7), 1771–1789.
- Cresswell, A.K., Edgar, G.J., Stuart-Smith, R.D., Thomson, R.J., Barrett, N.S. & Johnson, C.R. (2017) Translating local benthic community structure to national biogenic reef habitat types. *Global Ecology and Biogeography*, 26(10), 1112–1125. [10.1111/geb.12620](https://doi.org/10.1111/geb.12620).
- Dickie, L.M., Keer, S.R. & Boudreau, P.R. (1987) Size-dependent processes underlying regularities in ecosystem structure. *Ecological Monographs*, 57(3), 233–250.
- Dulvy, N.K., Polunin, N.V., Mill, A.C. & Graham, N.A. (2004) Size structural change in lightly exploited coral reef fish communities: evidence for weak indirect effects. *Canadian Journal of Fisheries and Aquatic Sciences*, 61(3), 466–475.
- Edgar, G.J. (1994) Observations on the size-structure of macrofaunal assemblages. *Journal of Experimental Marine Biology and Ecology*, 176(2), 227–243.
- Edgar, G.J., Cooper, A., Baker, S.C., Barker, W., Barrett, N.S., Becerro, M.A., (2020) Establishing the ecological basis for conservation of shallow marine life using Reef Life Survey. *Biological Conservation* 252, 2020.
- Edgar, G.J. & Shaw, C. (1995) The production and trophic ecology of shallow-water fish assemblages in southern Australia II. Diets of fishes and trophic relationships between fishes and benthos at Western Port, Victoria. *Journal of Experimental Marine Biology and Ecology*, 194(1), 83–106.
- Edgar, G.J. & Stuart-Smith, R.D. (2014) Systematic global assessment of reef fish communities by the Reef Life Survey program. *Scientific Data*, 1, 1–8.
- Edgar, G.J., Stuart-Smith, R.D., Willis, T.J., Kininmonth, S., Baker, S.C., Banks, S. et al. (2014) Global conservation outcomes depend on marine protected areas with five key features. *Nature*, 506(7487), 216–220.
- Fraser, K.M., Stuart-Smith, R.D., Ling, S.D. & Edgar, G.J. (2021) Small invertebrate consumers produce consistent size spectra across reef habitats and climatic zones. *Oikos*, 130(1), 156–170. <https://onlinelibrary.wiley.com/doi/10.1111/oik.07652>.
- Gillooly, J.F., Charnov, E.L., West, G.B., Savage, V.M. & Brown, J.H. (2002) Effects of size and temperature on developmental time. *Nature*, 417(6884), 70–73. <http://www.nature.com/articles/417070a>.
- Graham, N.A.J., Dulvy, N.K., Jennings, S. & Polunin, N.V.C. (2005) Size-spectra as indicators of the effects of fishing on coral reef fish assemblages. *Coral Reefs*, 24(1), 118–124.
- Heather, F.J., Blanchard, J.L., Edgar, G.J., Trebilco, R. & Stuart-Smith, R.D. (2021) Globally consistent reef size spectra integrating fishes and invertebrates. *Ecology Letters*, 24(3), 572–579. <https://onlinelibrary.wiley.com/doi/10.1111/ele.13661>
- Hebbali, A. (2020) olsrr: tools for building OLS regression models. R package version 0.5.3. <https://CRAN.R-project.org/package=olsrr>
- Hixon, M.A. & Beets, J.P. (1989) Shelter characteristics and Caribbean fish assemblages: experiments with artificial reefs. *Bulletin of Marine Science*, 44, 15.
- Hixon, M.A. & Beets, J.P. (1993) Predation, prey refuges, and the structure of coral-reef fish assemblages. *Ecological Monographs*, 63(1), 77–101. <https://doi.org/10.2307/2937124>.
- Jennings, S. & Blanchard, J.L. (2004) Fish abundance with no fishing: predictions based on macroecological theory. *Journal of Animal Ecology*, 73(4), 632–642. <http://doi.wiley.com/10.1111/j.0021-8790.2004.00839.x>.
- Jennings, S., Pinnegar, J.K., Polunin, N.V.C. & Boon, T.W. (2001) Weak cross-species relationships between body size and trophic level belie powerful size-based trophic structuring in fish communities. *Journal of Animal Ecology*, 70(6), 934–944.
- Kleiber, M. (1932) Body size and metabolism. *Hilgardia: A Journal of Agricultural Science*, 6(11), 315–353.
- Koenker, R. & Park, B.J. (1994) An interior point algorithm for non-linear quantile regression. *Journal of Econometrics*, 71(1–2), 265–283.
- Lindeman, R.L. (1942) The trophic dynamic of ecology. *Ecology*, 23(4), 399–417.
- Menge, B.A. & Lubchenco, J. (1981) Community organization in temperate and tropical rocky intertidal habitats: prey refuges in

- relation to consumer pressure gradients. *Ecological Monographs*, 51(4), 429–450. [10.2307/2937323](https://doi.org/10.2307/2937323).
- Nash, K.L. & Graham, N.A. (2016) Ecological indicators for coral reef fisheries management. *Fish and Fisheries*, 17(4), 1029–1054.
- Petchey, O.L. & Belgrano, A. (2010) Body-size distributions and size-spectra: universal indicators of ecological status? *Biology Letters*, 6(4), 434–437. <https://royalsocietypublishing.org/doi/10.1098/rsbl.2010.0240>.
- Peters, R.H. (1983) *The ecological implications of body size*. 2, Cambridge: Cambridge University Press.
- Platt, T. & Denman, K. (1977) Organisation in the pelagic ecosystem. *Helgoländer Wissenschaftliche Meeresuntersuchungen*, 30(1–4), 575–581.
- R Core Team (2020) R: A Language and Environment for Statistical Computing. <https://www.R-project.org/>
- Robinson, J.P.W., Baum, J.K. & Giacomini, H. (2016) Trophic roles determine coral reef fish community size structure. *Canadian Journal of Fisheries and Aquatic Sciences*, 73(4), 496–505. <http://www.nrcresearchpress.com/doi/10.1139/cjfas-2015-0178>.
- Robinson, J.W., Williams, I.D., Edwards, A.M., McPherson, J., Yeager, L.A., Vigliola, L. et al. (2017) Fishing degrades size structure of coral reef fish communities. *Global Change Biology*, 23(3), 1009–1022.
- Rogers, A., Blanchard, J.L. & Mumby, P.J. (2014) Vulnerability of coral reef fisheries to a loss of structural complexity. *Current Biology*, 24(9), 1000–1005. <https://doi.org/10.1016/j.cub.2014.03.026>.
- Rossberg, A.G., Gaedke, U. & Kratina, P. (2019) Dome patterns in pelagic size spectra reveal strong trophic cascades. *Nature Communications*, 10(1), 1–11. <https://doi.org/10.1038/s41467-019-12289-0>.
- Schmidt-Nielsen, K. & Knut, S.-N. (1984) *Scaling: why is animal size so important?* Cambridge: Cambridge University Press.
- Schwinghamer, P. (1981) Characteristic size distributions of integral benthic communities. *Canadian Journal of Fisheries and Aquatic Sciences*, 38(10), 1255–1263.
- Sheldon, R.W., Prakash, A. & Sutcliffe, W.H. (1972) The size distribution of particles in the ocean. *Limnology and Oceanography*, 17, 327–340.
- Shin, Y.J., Rochet, M.J., Jennings, S., Field, J.G. & Gislason, H. (2005) Using size-based indicators to evaluate the ecosystem effects of fishing. *ICES Journal of Marine Science*, 62(3), 384–396.
- Shulman, M.J. (1985) Coral reef fish assemblages: intra- and inter-specific competition for shelter sites. *Environmental Biology of Fishes*, 13(2), 81–92. <http://link.springer.com/10.1007/BF00002576>.
- Sprules, W.G. & Barth, L.E. (2016) Surfing the biomass size spectrum: Some remarks on history, theory, and application. *Canadian Journal of Fisheries and Aquatic Sciences*, 73(4), 477–495.
- Sprules, W.G., Casselman, J.M. & Shuter, B. (1983) Size distribution of pelagic particles in lakes. *Canadian Journal of Fisheries and Aquatic Sciences*, 40(10), 1761–1769. <http://www.nrcresearchpress.com/doi/10.1139/f83-205>.
- Sprules, W.G. & Munawar, M. (1986) Plankton size spectra in relation to ecosystem productivity, size, and perturbation. *Canadian Journal of Fisheries and Aquatic Sciences*, 43(9), 1789–1794. <http://www.nrcresearchpress.com/doi/10.1139/f86-222>.
- Stewart, B. & Beukers, J. (2000) Baited technique improves censuses of cryptic fish in complex habitats. *Marine Ecology Progress Series*, 197, 259–272. <http://www.int-res.com/abstracts/meps/v197/p259-272/>.
- Trebilco, R., Baum, J.K., Salomon, A.K. & Dulvy, N.K. (2013) Ecosystem ecology: size-based constraints on the pyramids of life. *Trends in Ecology & Evolution*, 28(7), 423–431. <https://doi.org/10.1016/j.tree.2013.03.008>.
- Trebilco, R., Dulvy, N.K., Stewart, H. & Salomon, A.K. (2015) The role of habitat complexity in shaping the size structure of a temperate reef fish community. *Marine Ecology Progress Series*, 532, 197–211.
- Tyberghein, L., Verbruggen, H., Pauly, K., Troupin, C., Mineur, F. & De Clerck, O. (2012) Bio-ORACLE: a global environmental dataset for marine species distribution modelling: Bio-ORACLE marine environmental data rasters. *Global Ecology and Biogeography*, 21(2), 272–281. <http://doi.wiley.com/10.1111/j.1466-8238.2011.00656.x>.
- Willis, T.J. (2001) Visual census methods underestimate density and diversity of cryptic reef fishes. *Journal of Fish Biology*, 59(5), 1408–1411. <http://doi.wiley.com/10.1111/j.1095-8649.2001.tb00202.x>.
- Wilson, S., Fisher, R., Pratchett, M., Graham, N., Dulvy, N., Turner, R. et al. (2010) Habitat degradation and fishing effects on the size structure of coral reef fish communities. *Ecological Applications*, 20(2), 442–451.
- Yamanaka, T., White, P.C.L., Spencer, M. & Raffaelli, D. (2012) Patterns and processes in abundance-body size relationships for marine benthic invertebrates. *Journal of Animal Ecology*, 81(2), 463–471. <https://doi.org/10.1111/j.1365-2656.2011.01921.x>.

SUPPORTING INFORMATION

Additional supporting information may be found online in the Supporting Information section.

How to cite this article: Heather, F.J., Stuart-Smith, R.D., Blanchard, J.L., Fraser, K.M. & Edgar, G.J. (2021) Reef communities show predictable undulations in linear abundance size spectra from copepods to sharks. *Ecology Letters*, 24, 2146–2154. <https://doi.org/10.1111/ele.13844>